

Supporting Information

Zhang et al. 10.1073/pnas.1016220108

SI Materials and Methods

Reagents. CTX (monohydrate, C0678) was purchased from Sigma-Aldrich; carboplatin (18742SE; 10 mg/mL) was purchased from Hospira U.K., and sunitinib malate was purchased from LC Laboratories (S-8803). Murine B16 melanoma and genetically manipulated and nonmanipulated T241 fibrosarcoma cells were cultured in DMEM supplemented with 10% FBS, 4 mM L-glutamine, and 1% penicillin-streptomycin.

Animals. C57/Bl6 mice were obtained from the local animal facility of the Department of Microbiology, Cell and Tumor Biology, Karolinska Institute. All animal experiments were approved by the North Stockholm Animal Board (Stockholm, Sweden).

Murine Tumor Models and Therapy. Approximately 1×10^6 C57/Bl6 tumor cells were s.c. injected into the middorsal region of each 6- to 8-wk-old C57/Bl6 mouse. Tumor-bearing mice began to receive treatment at the time point when the average tumor size reached 0.5–0.8 cm³. CTX at the dose of 62.5 mg/kg per day i.p., carboplatin at the dose of 50 mg/kg per day i.p., and sunitinib at the dose of 60 mg/kg per day p.o. were used for daily treatment as previously described standard dosages of these drugs (1–3). Monotherapy, simultaneous or sequential combinations of sunitinib with or without chemotherapy were designed as therapeutic regimens. Solvent buffer at the same volume was used as control in all experiments. Tumor sizes were measured every other day and calculated according to a standard formula ($\text{length} \times \text{width}^2 \times 0.52$) as previously described (4). In some experiments, mouse body weights were measured at the indicated time points. Mouse survival was closely monitored (at least three times per day) during the entire experimental period.

Whole-Mount Staining. Fresh tumor tissues were harvested and fixed in freshly prepared 4% paraformaldehyde for 24 h. Whole-mount staining was performed as previously described (5). Briefly, tumor tissues from nonnecrotic regions were cut into small pieces, digested with proteinase K (20 µg/mL) for 5 min, and subsequently treated with 100% methanol for 30 min at RT. Nonspecific binding sites were blocked overnight at 4 °C using a blocking buffer (3% skim milk in PBS containing 0.3% Triton X-100, PBST). Tissue sections were incubated overnight at 4 °C with a rat antimouse CD31 antibody (1:400 dilution in blocking buffer; PECAM-1, MEC 13.3, BD Bioscience 553370). Tissues

were rigorously washed with PBST four times, with each wash lasting for ~0.5 h). Tumor tissues were further blocked using the blocking buffer for an additional 2 h before incubation with the secondary antibody. An Alexa 555-labeled goat antirat secondary antibody (1:400 dilution in blocking buffer; Invitrogen, A21424) was incubated with tissues at RT for 2 h, followed by washing with PBST twice. Stained tissue sections were mounted with a Vectashield mounting medium (Vector Laboratories) and were analyzed by confocal microscopy (Zeiss Confocal LSM510 microscope; Carl Zeiss) or Nikon C1 Confocal microscope (Nikon). Tumor vascular density was quantified using six to eight random fields at 10× or 20× from four to five tumors per group.

H&E Staining. Paraffin-embedded bones from tumor-bearing and non-tumor-bearing mice were sectioned in 4-µm-thick sections and stained with H&E according to a standard method (6). Representative areas of BM were captured under a light microscope (20 × magnification).

Blood Chemistry. Peripheral blood of tumor-bearing and non-tumor-bearing mice were collected from the tail vein; 20 µL blood from each mouse was subjected to analysis using an auto-hematology analyzer (BC-2800 Vet, Mindray).

Statistical Analysis. For quantitative analysis, at least six to eight randomized micrographs from different fields were used. The Adobe Photoshop CS4 software program was used with a color range tool and a count tool to detect positive areas or numbers. Statistical analyses were performed using the standard two-tailed Student *t* test, and values of $P < 0.05$, $P < 0.01$, and $P < 0.001$ were considered statistically significant.

Beneficial Mechanism of Combination Therapy. Although tumor-produced VEGF acts locally to promote tumor neovascularization, it enters into the circulation to suppress BM hematopoiesis. ADs blocks VEGF-induced hematopoietic defects and thus increase tolerance of chemotoxicity. The clinical consequence is that delivery of chemotherapy to cancer patients who have impaired BM hematopoiesis or myelogenesis may lead to a high rate of therapy-induced mortality. Conversely, improvement of BM hematopoiesis and functions of other organs by ADs may significantly prevent chemotoxicity, leading to improved survival.

1. Egorin MJ (2008) Population pharmacokinetic/pharmacodynamic modeling of paclitaxel and carboplatin in ovarian cancer. *Clin Cancer Res* 14:2517, author reply 2517–2518.
2. Hayes DF, et al.; Cancer and Leukemia Group B (CALGB) Investigators (2007) HER2 and response to paclitaxel in node-positive breast cancer. *N Engl J Med* 357:1496–1506.
3. Motzer RJ, et al. (2007) Sunitinib versus interferon alfa in metastatic renal-cell carcinoma. *N Engl J Med* 356:115–124.

4. Cao R, et al. (1999) Suppression of angiogenesis and tumor growth by the inhibitor K1-5 generated by plasmin-mediated proteolysis. *Proc Natl Acad Sci USA* 96:5728–5733.
5. Björndahl M, et al. (2005) Insulin-like growth factors 1 and 2 induce lymphangiogenesis in vivo. *Proc Natl Acad Sci USA* 102:15593–15598.
6. Eriksson A, et al. (2002) Placenta growth factor-1 antagonizes VEGF-induced angiogenesis and tumor growth by the formation of functionally inactive PIGF-1/VEGF heterodimers. *Cancer Cell* 1:99–108.

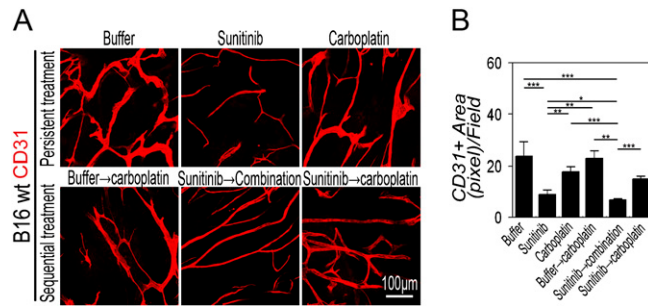


Fig. S1. Tumor vasculature of melanoma. (A) Tumor tissues from B16 melanoma tumor-bearing mice received monotherapy or sequential combination therapy were stained with CD31. Data are representative of two independent experiments with four to five tumors per group. (Bar = 100 μm .) (B) Quantification of tumor vascular density (10 \times , six to eight fields per group). Similar results were obtained from two independent experiments. * $P < 0.05$, ** $P < 0.01$, *** $P < 0.001$. Data are shown as mean \pm SEM.

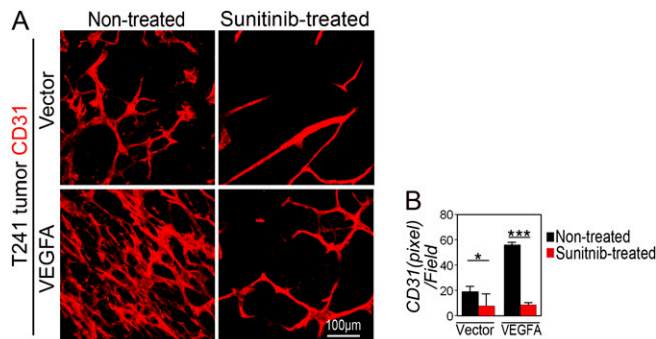


Fig. S2. Tumor vasculature of sunitinib-treated and nontreated T241 tumors. (A) Tumor tissues from VEGF- or vector-T241 tumor-bearing mice that received sunitinib or vehicle were stained with CD31. Data are representative of two independent experiments with four to five tumors per group. (Bar = 100 μm .) (B) Quantification of tumor vascular density (20 \times , six to eight fields per group). Similar results were obtained from two independent experiments. * $P < 0.05$, *** $P < 0.001$. Data are shown as mean \pm SEM.

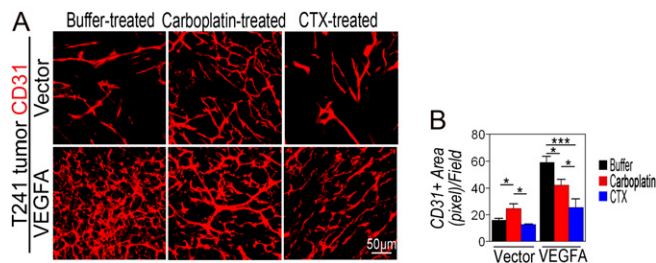


Fig. S3. Vasculatures of chemotherapy-treated T241 tumors. (A) Tumor tissues from VEGF- or vector-T241 tumor-bearing mice that received carboplatin, CTX, or vehicle were stained with CD31. Data are representative of two independent experiments with four to five tumors per group. (Bar = 50 μm .) (B) Quantification of tumor vascular density (20 \times , six to eight fields per group). Similar results were obtained from two independent experiments. * $P < 0.05$, *** $P < 0.001$. Data are shown as mean \pm SEM.

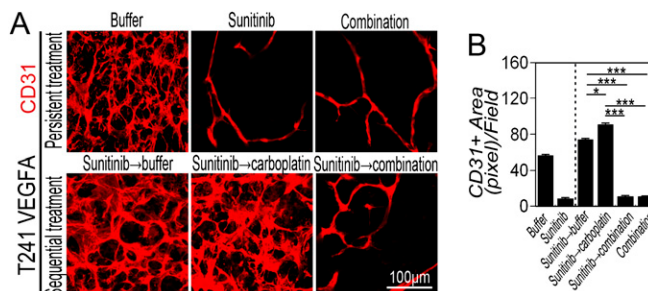


Fig. S4. Vasculatures of carboplatin-treated T241 tumors. (A) VEGF-T241 tumor-bearing mice received sunitinib monotherapy or combination of sunitinib plus carboplatin simultaneously or sequentially delivered. Tumor tissues were stained with CD31. Data are representative of two independent experiments with four to five tumors per group. (Bar = 100 μm .) (B) Quantification of tumor vascular density (20 \times , six to eight fields per group). Similar results were obtained from two independent experiments. * $P < 0.05$, *** $P < 0.001$. Data are shown as mean \pm SEM.

